19th Brazilian Congress of Thermal Sciences and Engineering
November 6th–10th, 2022, Bento Gonçalves - RS - Brazil

ENC-2022-0564
CFD SIMULATION OF RESPIRATORY DROPLETS AND AEROSOLS IN AIRFLOWS

Lucas P. Netto
Daniel J. N. M. Chalhub
Norberto Mangiavacchi
Department of Mechanical Engineering
Universidade do Estado do Rio de Janeiro, Rio de Janeiro, RJ, Brazil
lucaspereiranetto@gmail.com, daniel.chalhub@eng.uerj.br, norberto.mangiavacchi@eng.uerj.br

Abstract. *The COVID-19 pandemic raised the importance of breathing clean air in public establishments. High contamination of airborne diseases are expected during the winter, but recent studies does not indicate simple results. Some authors have approached the problem using Computational Fluid Dynamics (CFD) to simulate various scenarios to investigate different factors regarding the main cause of airborne disease transmission. However there is still not a consensus on how exactly is the mechanism of transmission. In this context, the present work uses CDF via software OpenFOAM to simulate the airflow and saliva particle dispersion on an event of a human cough. The model considers an Eulerian-Lagrangian method to track individual droplets of saliva in the airflow in a two-dimensional domain.*
Keywords: *CFD, Bioaerosols, Airborne pathogens, Particle tracking*

1. INTRODUCTION

The COVID-19 pandemic raised the importance of breathing clean air in public establishments. It is well known that airborne diseases, such as influenza, show a higher contamination rate in winter and cold weather in general due to bad air circulation. The work of Wood *et al.* (2014) indicates that re-breathed air is considerably higher at winter due to people spending more time indoors. It is claimed in the same article that the average re-breathed air while indoors does not differs. Conversely, airborne diseases' transmission is not scientifically understood, since recent studies on the topic do not indicate simple results. Despite Beaussier *et al.* (2022) and Hedworth *et al.* (2021) investigating the same problem, their results are highly dependent on their specific geometry.

Some authors have performed computational fluid dynamics (CFD) simulations to study various scenarios using different approaches. Dbouk and Drikakis (2020) calculates the distance saliva can reach in an event of a single cough, considering a multi-phase turbulent flow with an evaporation model for the respiratory aerosol. They use empirical data to provide the initial cough speed and the mouth geometry in their setup. Hedworth *et al.* (2021) uses the transport equation (Versteeg and Malalasekera, 1995) to evolve saliva concentration throughout the domain. This method of saliva dispersion is not optimal (Scharfman *et al.*, 2016), but is sufficient for the complexity of the problem, in which is considered a turbulent flow with the effect of HVAC system over a large domain.

The present work uses CFD to simulate the airflow and saliva particle dispersion on an event of a cough over the first 10 seconds of the simulation in a 2D domain. A simple physical model is implemented, reducing computational cost as compared to the works previously mentioned. This simpler approach's validity is also investigated.

2. PROBLEM FORMULATION

The problem uses an Eulerian-Lagrangian method to track individual droplets of saliva in an airflow. This method is used over a multi-phase approach to simplify the physical modeling and because of its fidelity (Mpagazehe, 2013). The fluid phase continuity and momentum equations are solved on an Eulerian grid. The fluid (air) is considered to be incompressible, since the flow occurs in outdoor space at low velocities, in which the Mach number is less than 0.1. Hence, the governing equations are the following:

$$\nabla \cdot \vec{u} = 0 \tag{1}$$

$$\frac{\partial \vec{u}}{\partial t} + \vec{u} \cdot \nabla \vec{u} = -\nabla p + \nu \nabla^2 \vec{u} + \vec{g} \tag{2}$$

where (1) is the mass continuity equation for incompressible fluids and (2) is the momentum equation for an incompressible Newtonian fluid (Versteeg and Malalasekera, 1995). In (1) and (2), $\vec{u}$, p, ν and $\vec{g}$ are the fluid's velocity, pressure, kinematic viscosity and the acceleration due to gravity, respectively.

The saliva droplets are considered to be simple particles with motion governed by Newton's second law, thus following the Lagrangian approach. Each individual particle is considered to be a water sphere with no particle-particle collision, and are subjected to weight, buoyancy and drag forces (Fox *et al.*, 2020).

$$\frac{d\vec{u_p}}{dt} = \left(1 - \frac{\rho_f}{\rho_p}\right)\vec{g} + \frac{6\vec{F}_D}{d^3\pi\rho_p} \tag{3}$$

where $\vec{u_p}$ is the particle velocity, d is the particle diameter, ρ_p is the particle (water) density, ρ_f is the fluid (air) density and $\vec{F}_D$ is the drag force. The later is described in (4):

$$\vec{F}_D = \frac{1}{8}\rho_f C_D |\vec{u} - \vec{u_p}|(\vec{u} - \vec{u}_p)\pi d^2 \tag{4}$$

The drag coefficient C_D is a function of the Reynolds Number (Re) on a sphere (Sharifi *et al.*, 2020), and both are given by:

$$\mathrm{Re} = \frac{|\vec{u} - \vec{u}_p|d}{\nu} \tag{5}$$

$$C_D(\mathrm{Re}) = \begin{cases} 0.424, & \mathrm{Re} > 1000 \\ \frac{24}{\mathrm{Re}}\left(1 + \frac{1}{6}\mathrm{Re}^{\frac{2}{3}}\right), & \mathrm{Re} \leq 1000 \end{cases} \tag{6}$$

The ambient is considered to be at a constant temperature of 25°C. Therefore, the air kinematic viscosity and density, and water density are considered $\nu = 1.562 \times 10^{-5}$ m^2/s, $\rho_f = 1.184$ kg/m^3 and $\rho_p = 997$ kg/m^3, respectively (Boles and Cengel, 2014).

The configuration of the problem depends on some parameters that characterize the goal of the simulation. These parameters are: Initial cough velocity, cough period, and saliva droplets' diameter distribution. The velocity is modeled to be a piece-wise function, with a constant flow for the duration of the cough and no flow after that. Kwon *et al.* (2012) show that the average cough initial velocity is $u_0 = 15.3$ m/s, and Dbouk and Drikakis (2020) use a cough period of 0.12 seconds. Therefore it is imposed a time-dependent boundary condition for the velocity at the mouth as follows:

$$u_x(t) = \begin{cases} u_0, & t \leq 0.12 \\ 0, & t > 0.12 \end{cases} \tag{7}$$

The Normal Distribution was considered in order to estimate the size of the droplets exiting the mouth during the simulation. The diameters of the droplets range between 60 and 100 μm, with mean value of 75 μm and a standard deviation of 25 μm (Carboni, 2020; Xie *et al.*, 2007). In an event of a cough, Dbouk and Drikakis (2020) predicts that, on average, it is produced 7.7 mg of free water particles. With these information, it is possible to define the estimated number of individual particles exiting the mouth, as well as the number of particles per second during the event. It is worth noting that the saliva cloud initial velocity is the same as the air leaving the mouth and entering the computational domain.

The simulation geometry is a two-dimensional domain of a rectangle with a length of $L = 3.6$ m and a height of $H = 3$ m, where a sketch of a person sits inside of it, as seen in Fig. 1. The person's mouth is modeled to be a simple line of 16 mm.

Fig. 2 shows the boundary conditions on the domain: at the Free boundary it is imposed $\vec{n} \cdot \nabla\vec{u} = 0$ and a hydrostatic pressure gradient $p = -g(y - H)$, where $g = 9.81$m/s^2, H is the height of the domain, and $\vec{n}$ is the unit normal vector to the surface. It is imposed $\nabla p = 0$ and (7) at the mouth. For the floor and the human it is imposed the no-slip condition for the velocity and $\nabla p = 0$ for the pressure. Initial conditions for the simulations are $\vec{u} = 0$ and $p = 0$ in the whole domain.

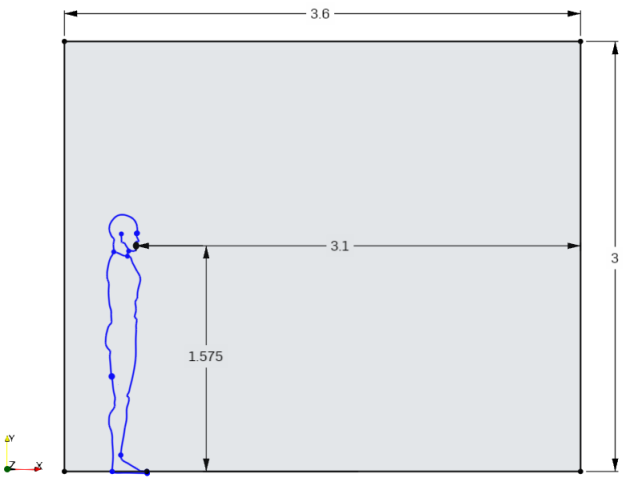

Figure 1: CAD of the domain. The mouth is modeled to be roughly 1.6 m high and 3.1 m away from the right edge. Coello (2008) published the human sketch file online.

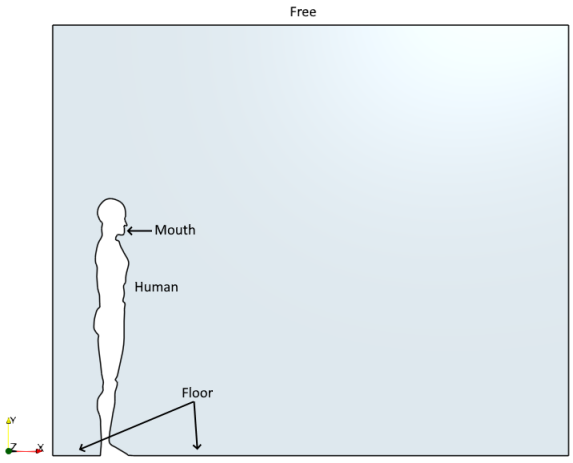

Figure 2: Specified boundaries of the domain. The left, right and upper edges of the rectangle are conjoined into a single boundary named "Free".The boundary specified as "Human" is the entire human sketch without "Mouth".

3. RESULTS AND DISCUSSION

The geometry was first modeled using Onshape, a free CAD software with cloud processing (Flaherty, 2022). Since OpenFOAM does not support two-dimensional mesh files, the sketch was extruded 0.01 m in the Z direction to form a three-dimensional STEP file. The STEP file was then imported to Salome, a free multi-functional software aimed to aid pre- and pos-processing of numerical simulations. SMesh, a meshing Salome tool, was used to subdivide the domain, showed in Fig. 3. The algorithm NETGEN 1D-2D (CASCADE, 2012) was used to generate the mesh, which ensures a refined mesh near the mouth (see Fig. 2) and a coarser mesh far from the mouth.

The solution of the equations (1), (2) and (3) is given by OpenFOAM v1912 software, using the Eulerian-Lagrangian solver DPMFoam. OpenFOAM uses the finite volume method to converge the partial differential equations' solution in the entire domain over discrete time steps. For this simulation, a dynamic time step model was used to keep the maximum Courant number below 0.4 at every time step.

3.1 Mesh

A mesh independence analysis was conducted before choosing an appropriate grid to run the simulation. The procedure to calculate the Grid Convergence Index (GCI) of a key parameter, proposed by Celik *et al.* (2008), was used as a criteria to determine the validity of the numerical solution. Fig. 3a shows a previous generated mesh, which upon several steps of mesh refinement (4 steps in total) lead to Fig. 3b.

Table 1 shows the calculation of errors due to discretization over 3 increasingly refined meshes (N1, N2, N3). ϕ is defined as the average u_x evaluated at a vertical line 0.3 m away from the mouth at $t = 0.1$ s and $t = 0.2$ s. The numerical uncertainty of each ϕ as the mesh is refined is given by GCI^{21}_{fine} and GCI^{32}_{fine}.

It is possible to conclude that, although at $t = 0.1$ s a $GCI^{21}_{fine} = 2.22\%$ is achieved, the parameter ϕ at $t = 0.2$ indicates $GCI^{21}_{fine} = 11.15\%$, a high numerical uncertainty when refining from mesh N1 to N2. The Grid Convergence Index is below 2% for both parameters when refining from mesh N2 to N3, therefore N3 is used for this work.

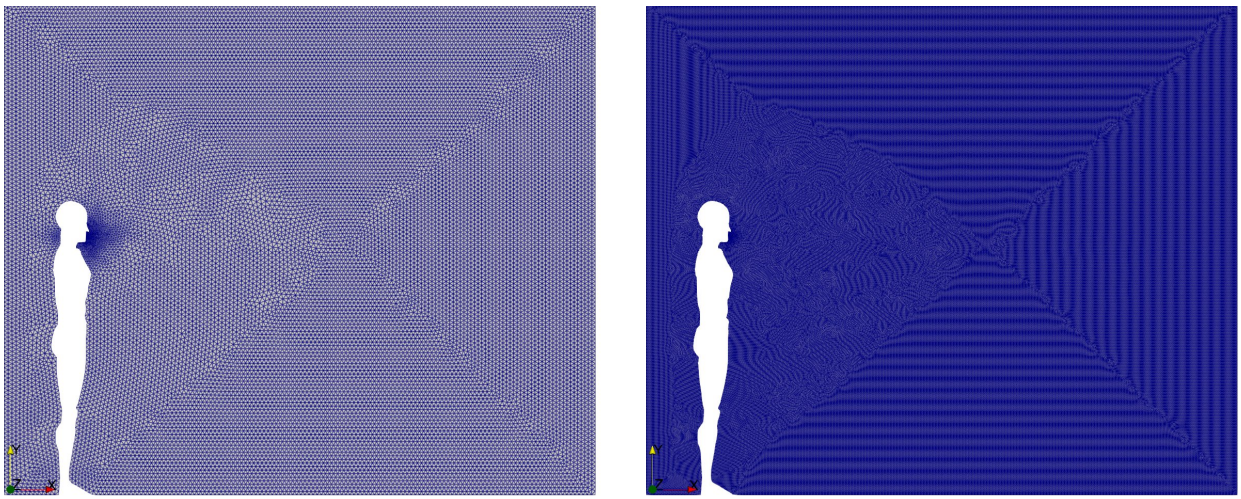

(a) (b)

Figure 3: 2D computational grid of the domain. Fig. 3a depicts a coarser mesh with 39722 elements, while 3b depicts N3: a finer mesh with 407730 elements.

Table 1: Mesh convergence strategy parameters, as proposed by (Celik *et al.*, 2008).

	ϕ for $t = 0.1$ s	ϕ for $t = 0.2$ s
N1, N2, N3	122295, 237970, 407730	122295, 237970, 407730
r_{21}	1.39494	1.39494
r_{32}	1.30896	1.30896
ϕ_1	0.0789564	0.0456973
ϕ_2	0.0808648	0.0602048
ϕ_3	0.0801431	0.0623613
p	2.58332	4.55731
ϕ^{21}_{ext}	0.0775561	0.04162
ϕ^{32}_{ext}	0.081583	0.0593103
e^{21}_{a}	2.42%	31.75%
e^{32}_{a}	0.89%	3.58%
e^{21}_{ext}	1.81%	9.80%
e^{32}_{ext}	0.88%	1.51%
GCI^{21}_{fine}	2.22%	11.15%
GCI^{32}_{fine}	1.11%	1.86%

3.2 Numerical results

The results of the simulation, considering an end time of 10 second, are presented in this section. Five key times ($t = 0.1$ s, $t = 0.2$ s, $t = 1$ s, $t = 5$ s and $t = 10$ s) was extracted and depicted in Fig. 4 and Fig. 5.

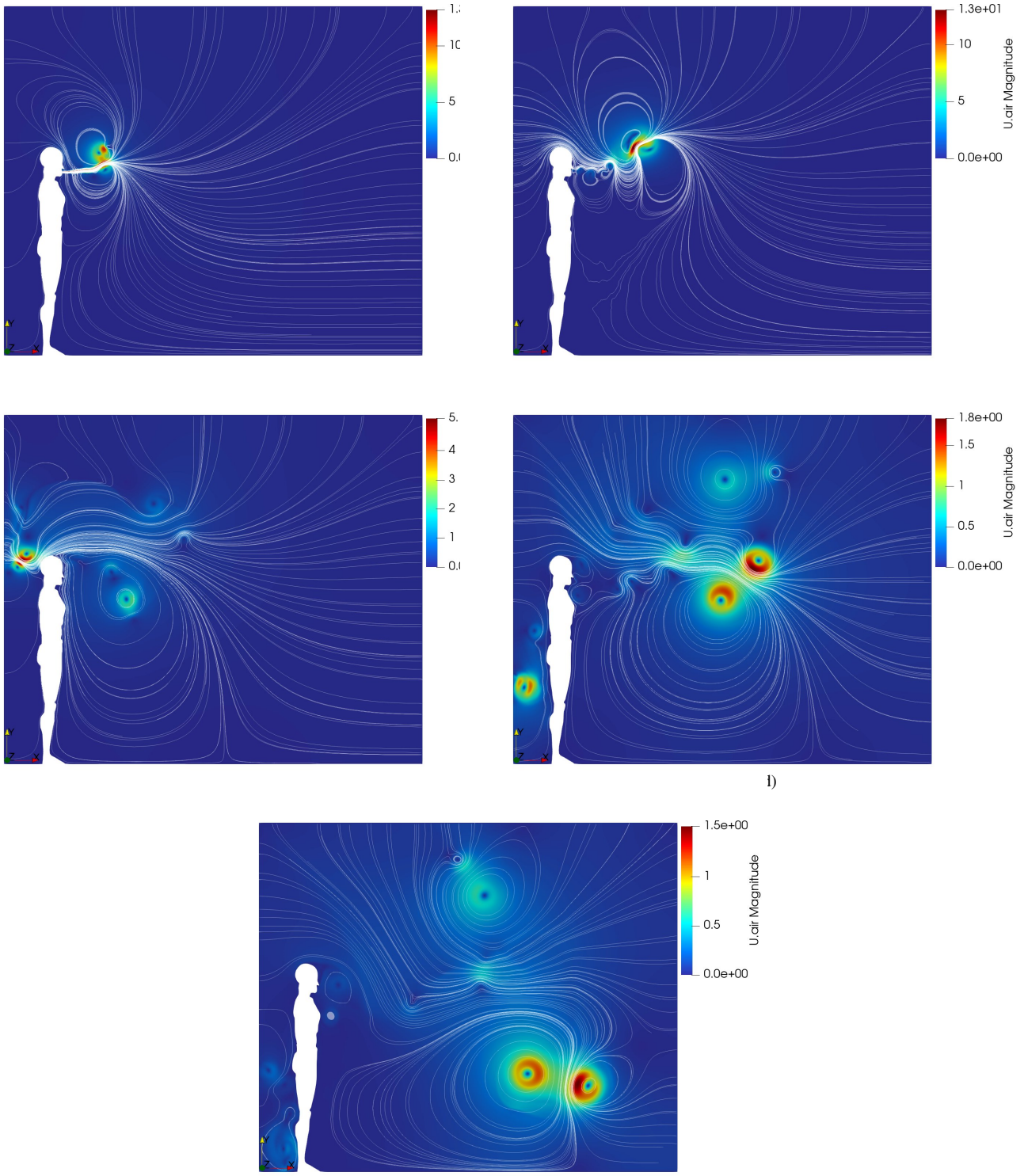

Figure 4: Streamline plots of the velocity field along with the velocity magnitude field over the domain. 4a, 4b, 4c, 4d and 4e are the simulation results at $t = 0.1$ s, $t = 0.2$ s, $t = 1$ s, $t = 5$ s and $t = 10$ s respectively.

Fig. 4a shows the velocity field and its streamline plot midway through the cough period. It is possible to see the formation of two vortexes due to the sudden initial cough velocity over a the domain with an uniform stationary fluid

(Santos and Anjos, 2020). Fig. 4b takes place right after the end of the cough time, which forms a region of turbulent fluid motion near the mouth. Fig. 4c, 4d and 4e shows the evolution of the many vortexes created by the high velocity cough.

Fig. 5 illustrate the particle position throughout the simulation. The diameter of each particle is color-plotted, showing that smaller particles that are inside the high velocity main stream tends to follow it, while the bigger ones are more influenced by their weight force in the first 0.2 s of the simulation. One can see that Figs. 4c and 4d show a vortex creating an upstream of air near the human's chest, which prevents the water droplets that were disjointed from the main high velocity flow to fall any further. Figs. 5e and 5f indicates that the final position of each individual water droplet depends more on the time it was generated during the cough than its diameter. A total number of 34994 Lagrangian particles were generated in the simulation.

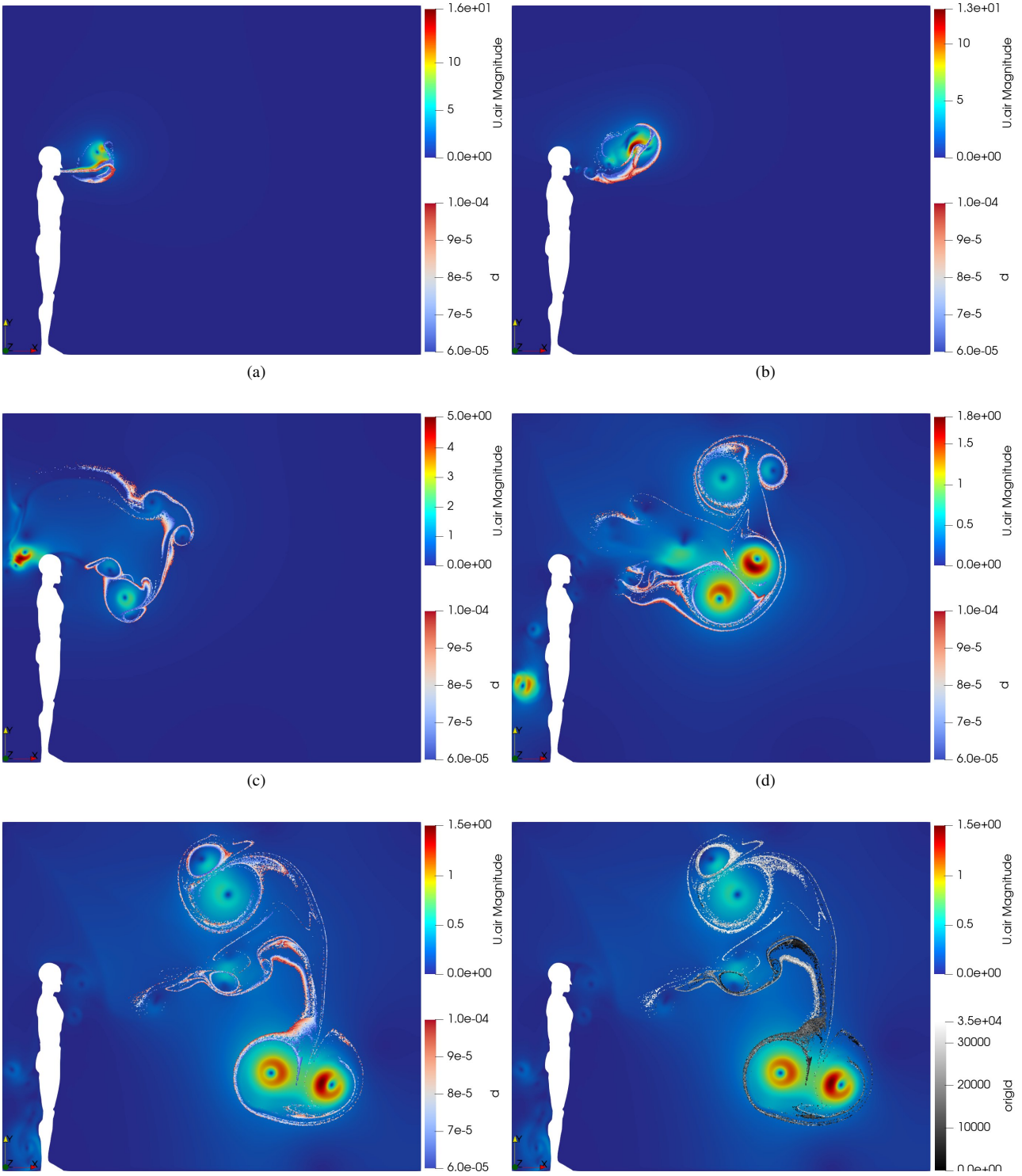

Figure 5: Diameter distribution of each water particle along with the velocity magnitude field over the domain. 5a, 5b, 5c, 5d and 5e are the simulation results at $t = 0.1$ s, $t = 0.2$ s, $t = 1$ s, $t = 5$ s and $t = 10$ s respectively. 5f represents particle's ID number in $t = 10$ s.

4. CONCLUSIONS

In this work, a numerical simulation of the first ten seconds of a coughing event was performed. The effects of the airflow in the saliva droplets was studied using the Eulerian-Lagrangian solver DPMFoam, where the influence of the particles' diameter was investigated.

Although, the two-dimensional model imply some limitations, the present study provides a good initial understanding of particle dispersion in a cough event. One of the limitations due to the 2D model is the blockage of the air by the human at the left portion of the domain. In other words, the air can only flow around the top of the human sketch. In addition, the presence of the vortex near the human's chest lead to a portion of the particles to rise, which could not be physically accurate in a scenario without any wind (Scharfman *et al.*, 2016). Despite the particles not interacting with each other, the uniform steady temperature and not using the water droplet evaporation model, the numerical results for the horizontal travel distance are consistent with the literature (Santos and Anjos, 2020; Dbouk and Drikakis, 2020) for the first second of a cough event.

It is possible that, for the problem proposed in this work, the Grid Convergence Index strategy used was not the most appropriate due to the chaotic nature of the simulation. Using a statistical approach could achieve better results using the methods mentioned in the works of Glimm and Sharp (1999) and Yu *et al.* (2006) for chaotic flows.

Simulations in three-dimensional domains, with geometries resembling realistic rooms, and different physical modeling, such as a multi-phase approach, will be studied and implemented in future works.

5. ACKNOWLEDGEMENTS

The authors would like to acknowledge financial support from FAPERJ, CNPq, CAPES, and UERJ.

6. REFERENCES

Beaussier, M., Vanoli, E., Zadegan, F., Peray, H., Bezian, E., Jilesen, J., Gandveau, G. and Gayraud, J.M., 2022. "Aerodynamic analysis of hospital ventilation according to seasonal variations. a simulation approach to prevent airborne viral transmission pathway during covid-19 pandemic". *Environment International*, Vol. 158, p. 106872.

Boles, M. and Cengel, Y., 2014. "Thermodynamics: An engineering approach". *New York: McGraw-Hil l Education*.

Carboni, G., 2020. *Numerical investigation of SARS-CoV-2 and atmospheric particulate deposition on the surface of the eye*. Master's thesis, UNIVERSITY OF GENOVA.

CASCADE, O., 2012. *SALOME documentation*. CEA/DEN, EDF R&D, OPEN CASCADE, 9th edition.

Celik, I.B., Ghia, U., Roache, P.J. and Freitas, C.J., 2008. "Procedure for estimation and reporting of uncertainty due to discretization in cfd applications". *Journal of fluids Engineering-Transactions of the ASME*, Vol. 130, No. 7.

Coello, A.E.G., 2008. "Human figures". `https://www.bibliocad.com/en/library/human-figures_26092/`. Accessed: 2022-06-18.

Dbouk, T. and Drikakis, D., 2020. "On coughing and airborne droplet transmission to humans". *Physics of Fluids*, Vol. 32, No. 5, p. 053310.

Flaherty, N., 2022. "Train the next generation with free cloud cad". https://www.onshape.com/en/resource-center/articles/train-the-next-generation-with-free-cloud-cad.

Fox, R.W., McDonald, A.T. and Mitchell, J.W., 2020. *Fox and McDonald's introduction to fluid mechanics*. John Wiley & Sons, Nashville, TN, 10th edition.

Glimm, J. and Sharp, D., 1999. "Prediction and the quantification of uncertainty". *Physica D: Nonlinear Phenomena*, Vol. 133, No. 1-4, pp. 152–170.

Hedworth, H.A., Karam, M., McConnell, J., Sutherland, J.C. and Saad, T., 2021. "Mitigation strategies for airborne disease transmission in orchestras using computational fluid dynamics". *Science Advances*, Vol. 7, No. 26, p. eabg4511.

Kwon, S.B., Park, J., Jang, J., Cho, Y., Park, D.S., Kim, C., Bae, G.N. and Jang, A., 2012. "Study on the initial velocity distribution of exhaled air from coughing and speaking". *Chemosphere*, Vol. 87, No. 11, pp. 1260–1264.

Mpagazehe, J.N., 2013. *A physics-based, Eulerian-Lagrangian computational modeling framework to predict particle flow and tribological phenomena*. Ph.D. thesis, Carnegie Mellon University.

Santos, D. and Anjos, G., 2020. "Numerical simulation of multiphase flows in the context of covid-19/sars-cov-2". doi:10.26678/ABCM.ENCIT2020.CIT20-0273.

Scharfman, B., Techet, A., Bush, J. and Bourouiba, L., 2016. "Visualization of sneeze ejecta: steps of fluid fragmentation leading to respiratory droplets". *Experiments in Fluids*, Vol. 57, No. 2, pp. 1–9.

Sharifi, K., Behbahani, T.J., Ebrahimi, S., Sabeti, M. and Soflaee, S., 2020. "A new computational fluid dynamics study of a liquid-liquid hydrocyclone in the two phase case for separation of oil droplets and water". *Brazilian Journal of Chemical Engineering*, Vol. 36, pp. 1601–1612.

Versteeg, H. and Malalasekera, W., 1995. "Computational fluid dynamics". *The finite volume method*, pp. 1–26.

Wood, R., Morrow, C., Ginsberg, S., Piccoli, E., Kalil, D., Sassi, A., Walensky, R.P. and Andrews, J.R., 2014. "Quan-

tification of shared air: a social and environmental determinant of airborne disease transmission". *PloS one*, Vol. 9, No. 9, p. e106622.

Xie, X., Li, Y., Chwang, A., Ho, P. and Seto, W., 2007. "How far droplets can move in indoor environments–revisiting the wells evaporation-falling curve." *Indoor air*, Vol. 17, No. 3, pp. 211–225.

Yu, Y., Zhao, M., Lee, T., Pestieau, N., Bo, W., Glimm, J. and Grove, J.W., 2006. "Uncertainty quantification for chaotic computational fluid dynamics". *Journal of Computational Physics*, Vol. 217, No. 1, pp. 200–216.

7. RESPONSIBILITY NOTICE

The authors are solely responsible for the printed material included in this paper.